Proceedings of the 10th World Congress on Mechanical, Chemical, and Material Engineering (MCM'24)
Barcelona, Spain - August 22-24, 2024
Paper No. ICMIE 157
DOI: 10.11159/icmie24.157

Topology-Lattice Optimization of an Extendable Wing

Altan Kayran[1], BuğraAksoy[2]
[1]Department of Aerospace Eng., Middle East Technical University
Ankara, Turkey
akayran@metu.edu.tr; bugra.aksoy@metu.edu.tr
[2] Turkish Aerospace Industries
Ankara, Turkey

Abstract **-** The main focus of this study is to develop a structural concept for an extendable wing for munition utilizing lattice cell assisted topology optimization followed by size optimization of the radii of the strut-based lattice cells. The topology optimization of the design space of the wing structure is performed using the Solid Isotropic Material with Penalization (SIMP) method for minimum compliance subject to volume fraction constraint. Depending on the relative density distribution, the topology optimized region is filled with strut-based lattice structures. Following the lattice assisted topology optimization, size optimizations for the radii of the lattice cells are performed using single and multi-objective functions. The resulting optimized wing structures are compared with each other in terms of their mechanical performances and weight. The results shows that the mechanical performance of the wing structure can be increased by employing lattice cell structures. Size optimizations performed using single and multi-objective functions also showed that the mechanical performances of the lattice assisted topology optimized wing structures are very close to each other and as a result of two level optimization approximately 17.5% weight reduction is achieved.

Keywords**:** Topology Optimization, Strut-based Lattice Structure, Multi-Objective Optimization, Extendable Wing, Additive Manufacturing

1. Introduction

NC milling is a widely used technique to manufacture metallic parts in the aerospace industry. However, it also has unique disadvantages such as scrap material and long machining time. Therefore, different manufacturing methods are recently developed such as additive manufacturing. Introducing additive manufacturing methods brings about new design techniques, structural configurations and results in improvement in mechanical performance of a structure. Lattice cell structures, a design of combination of struts or geometrical surfaces defined with mathematical expressions or plates, can be easily fabricated with additive manufacturing. In addition, different configurations of the lattice cell structures can be employed depending upon desired mechanical performance of structure. Example of strut-based lattice cell structures are given in Figure 1.

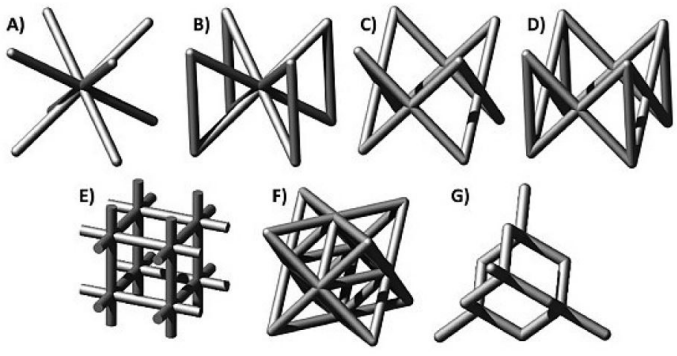

Fig 1: Example of strut-based lattice cell structures [1]

When lattice structures are examined at the cellular level, their behavior is governed by their type and material properties. However, when the structure formed by multiple lattice cell structures is examined at the overall structural level, these cells

behave like a homogenised meta-material [2]. By optimizing lattice parameters such as cell size, topology and strut diameters, the physical response of lattice structures can be improved in terms of acoustic [3] and mechanical performance [4]. In the literature, Dong et al. conducted a case study on the three point bending test specimen by using topology optimization utilizing the Bidirectional Evolutionary Structural Optimization (BESO) method to remove the unnecessary material and the removed area is filled with lattice structures [5]. As a follow-up study, size optimization study is conducted to determine the optimum dimensions of the lattice structure. The study concluded that lattice-solid hybrid structure resulted in improved critical buckling load and stiffness. Moreover, manufacturability of the lattice-solid hybrid structure is increased since lattice cells contributed as a support structure. Liu et al. conducted another design and optimization study on the spoiler of aircraft to improve its stiffness to weight ratio [6]. Initially, topology optimization is conducted on the structure. Having removed material with low relative densities, 3D kagome type lattice structures are implemented to support remaining solid elements. It is observed that final optimized structure has weight reduction and it can fulfill stress and displacement requirements. In 2018, Li et al. conducted research on the three point bending specimen by modeling gyroid based functionally graded cellular structures [7]. It is concluded that strength of the functionally graded cell structure is increased 161.9 percent compared to beam containing uniform lattice cell structure. In another study, topologically optimized three point bending specimen is combined with three different manually generated strut based lattice cell structure by Teimouri et al. [8]. According to the results, mechanical performance of three point bending specimen is increased in terms of stiffness, buckling failure load and energy absorption with lattice-solid hybrid design compared to only topologically optimized design. In addition to combination of lattice structures with topology optimization, different studies are conducted to increase mechanical performance of lattice structure with multi-objective optimization in terms of different objective functions.

In the present paper, a two level optimization strategy is followed for an extendable wing for munition. The optimization methodology is based on lattice cell assisted topology optimization followed by size optimization for lattice cells. Extendable wings are used for munitions to ensure that the munitions reach increase their range. Metallic wing structures of munitions are generally manufactured with NC milling. An example of munitions is demonstrated in Figure 2.

Fig. 2: Examples of expandable wings for munitions; JDAM-ER by Boeing [9]

In the present study, lattice cell assisted topology optimization is conducted to the extendable wing for minimum compliance. Strut-based lattice cells distributed in the design space based on the relative density distribution and the volume fraction constraint used. For the ease of manufacturability, strut radii of lattice cells are grouped under 5 different design variables and as a follow-up study single and multi-objective size optimizations are performed to determine the optimal radii for the 5 groups of strut-based lattice cells. In the strut radius optimization, compliance and mass are taken as separate objective functions and also combined in a multi-objective function.

2. Description of the Design and Non-Design Spaces and the Optimization Methodology

Before the topology optimization, design and non-design spaces are defined in the wing geometry. The wing structure is divided into three zones; the leading edge section (0- 0.25 chord), wing box section (0.25-0.75 chord) and trailing edge section (0.75 -1 chord). The wing box zone is defined as the design space where lattice structures are placed. Other zones are included into the non-design space. In order to distribute the lattice structure, widely known topology optimization

method, Solid Isotropic with Material Penalization (SIMP), is employed within the Hypermesh-Optistruct environment [10]. The finite element model of the wing structure is presented in Figure 3 with its skin panel and skin panel hidden. Figure 4 shows the cross-section of the finite element model of the wing where the design and non-design spaces are defined and element types are described. The yellow colored 3D elements in the wing box belong to the design space, where lattice structures are placed.

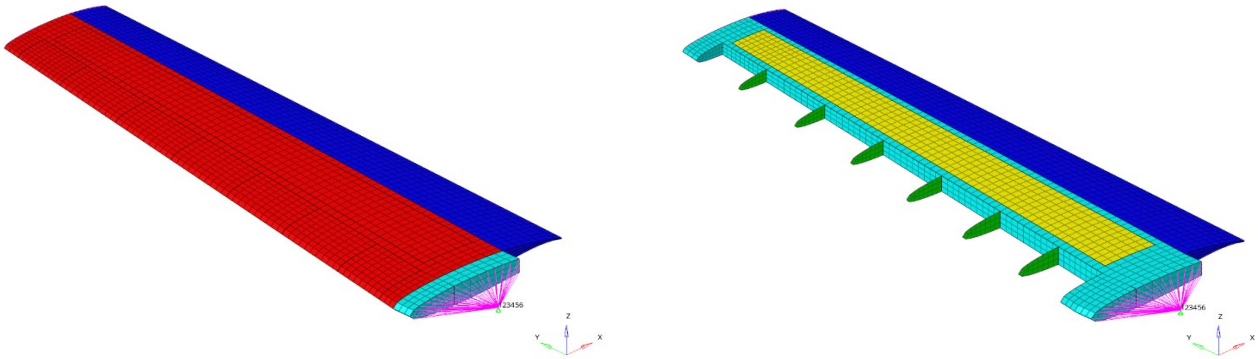

Fig. 3: Finite element model of the wing

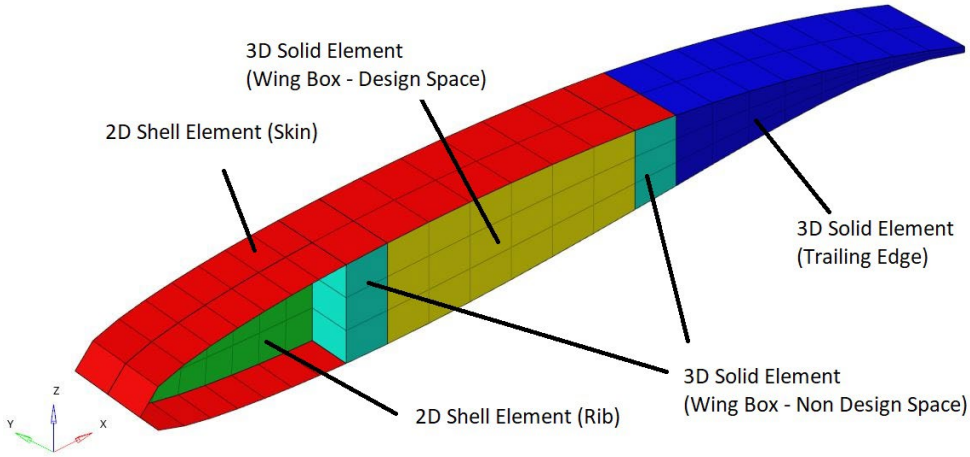

Fig. 4: The cross section of the finite element model of the wing

For the lattice placement, topology optimization parameters are defined in Equation 1,

$$\begin{gathered} Minimize\ C(\rho) \\ Subjected\ to \frac{V(\rho)}{V_0} \leq 0.5 \\ Fundamental\ Frequency \geq 21\ Hz \\ \sigma_{VM_{MAX}} \leq 165\ MPa \\ Lattice\ Placement\ if\ 10^{-6} \leq \rho \leq 0.4 \end{gathered} \tag{1}$$

where $C(\rho)$ is the compliance of the overall structure with respect to relative density, $V(\rho)$ is the volume of design space with respect to relative density, V_0 is the initial volume of design space, $\sigma_{VM_{MAX}}$ is the maximum von-Mises in the

wing structure, which is limited to 165 MPa. Another constraint is defined as the fundamental frequency, which is desired to be higher than 21 Hz. Upper and lower bounds of the relative density for the lattice placement is defined between 0.4 and 10^{-6}. During the topology optimization, following the relative density calculation in each iteration, if the relative density of the 3D element is lower than 0.4, 3D element is replaced with strut-based lattice structure, modeled with 1D beam elements. Otherwise, the 3D element remains as is. It should also be noted that in the wing structure, void is not desired to prevent the panel buckling. Therefore, the lower bound for the lattice placement is taken as 10^{-6}, so instead of void elements, lattice structures are placed. In addition, the upper bound is defined as 0.4 which is selected so as to make the post processing easy. When the strut radius is large relative to the unit cell size, during additive manufacturing powders may stick to each other especially in the corners, and this in turn causes weight penalty and makes the surface polishing difficult. Having completed topology optimization in Hypermesh-Optistruct, relative densities for each element are determined. Depending on the relative density distribution, lattice structures are placed in HyperMesh automatically and radii of the struts of lattice cells are determined.

Having determined the lattice distribution based on the topology optimization, size optimization study is undertaken and the compliance and the mass of the wing structure is minimized separately. For size optimization, the strut radii of lattice cells are optimized via the HyperStudy [10], which requires a parameterized finite element file. For the strut radius optimization, radius value in the 1D beam element cards needs to be parameterized. In order to parametrize the lattice diameter and connect it to different design variables, a script is developed in Phyton language. This script basically finds the beam properties in the finite element model file and assigns the initial, maximum and minimum possible strut diameters. For the initial sizing process of the strut radii, optimization parameters and constraints are given in Equation 2,

$$\begin{gathered} Minimize\ C(\rho)\ or\ M(r) \\ V(r) \leq V_{topology\ optimized} \\ Fundamental\ Frequency \geq 21\ Hz \\ \sigma_{VM_{MAX}} \leq 165\ MPa \\ 0.15\ mm \leq r \leq 2\ mm \end{gathered} \tag{2}$$

where $C(r)$ and $M(r)$ are the compliance and mass of the wing in terms of strut radius, $\sigma_{VM_{MAX}}$ is the maximum von-Mises stress constraint, bounds of the strut radii are defined as 0.15- 2 mm, which are decided by considering the manufacturability issue and ease of post processing of the resulting structure, $V(r)$ is the total volume of the structure, which is limited to the volume of initially lattice placed structure obtained as a result of topology optimization ($V_{topology\ optimized}$). It should be noted that normally both stress and volume constraints are not necessarily used together with compliance or mass objective functions. However, in this optimization study, both of them are introduced since they are needed in the multi-objective optimization phase where both compliance and mass are minimized. In the multi objective optimization, normalized objective function is defined as given in Equation 3,

$$N(r) = W_1 * \frac{M(r) - M_{min}}{M_{max} - M_{min}} + W_2 \frac{C(r) - C_{min}}{C_{max} - C_{min}} \tag{3}$$

where W_1 and W_2 are the weight factors, which are taken as 0.5 since equal weight is desired for minimum compliance and mass, M_{min}, M_{max} are the minimum and maximum mass values and C_{min}, C_{max} are the minimum and maximum compliance values calculated with single objective optimization under the same constraint given in Equation 2.

3. Results

3.1. Topology Optimization with Lattice Placement

At the end of topology optimization for lattice placement, each lattice cell may have different strut radius depending on the relative density of the particular element. As a result of lattice cell assisted topology optimization for minimum compliance, the wing structure containing the strut based lattice cells is obtained as shown in Figure 5.

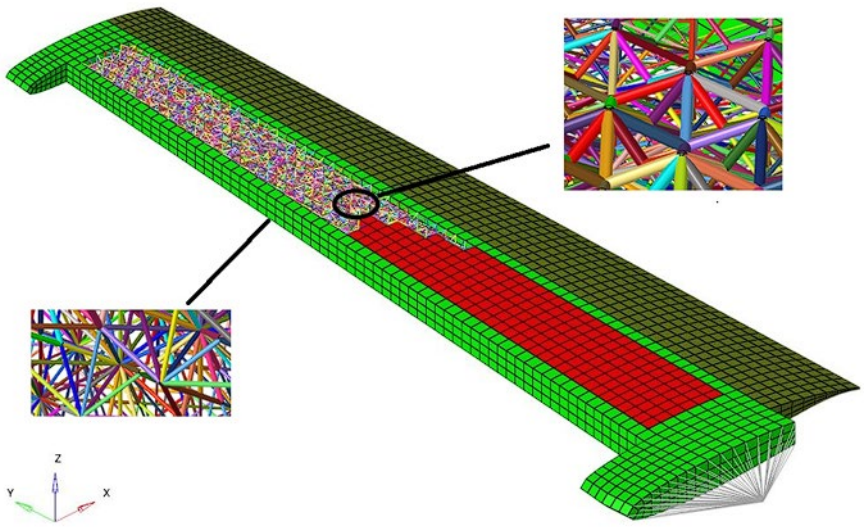

Fig. 5: Lattice placed wing structure obtained as a result of topology optimization for minimum compliance

The variation of the compliance and the frequency constraint with the iterations are given in Figure 6.

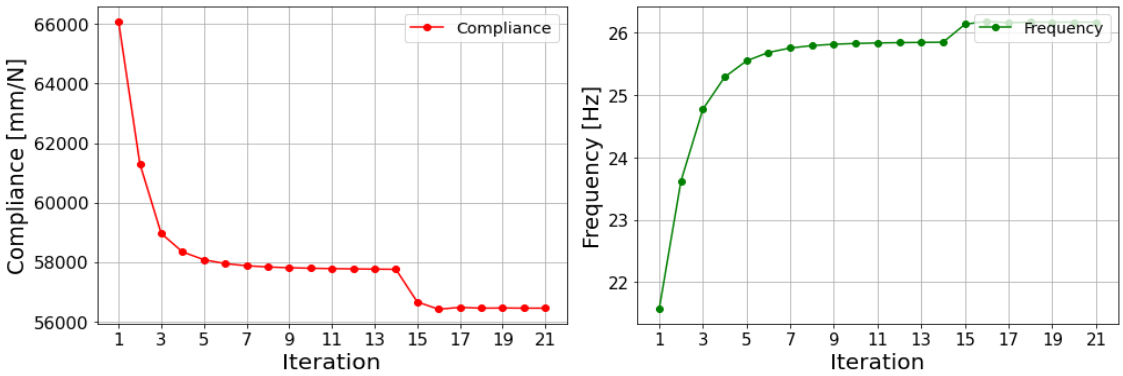

Fig. 6: Variation of compliance and the frequency constraint with iterations for the topology optimization with lattice placement

It should be noted that in the lattice cell assisted topology optimization performed in Hypermesh-Optistruct, volume fraction parameter used to determine the relative density distribution during the optimization does not initially account for lattice structures. Instead, lattice structures are added at the end of the topology optimization process based on the calculated relative densities. Consequently, the final volume of the lattice-placed structure tends to be higher than that of the structure optimized using only topology optimization. Additionally, in the lattice cell assisted topology optimization process, since lattice cells are placed following the topology optimization, stress constraint is only active for the 3D elements but not for the beams elements used to model the struts of lattice cells. Hence, follow-up lattice cell size optimization should be

conducted to provide lattice structures that do satisfy the imposed stress constraint. Before the size optimization, following the topology optimization, linear static and modal analyses are conducted on the lattice placed wing structure to evaluate the structural performance of the final topology optimized, lattice placed wing structure. As noted before, since lattice placement is done after the topology optimization, some of the responses can not be checked during the topology optimization such as the maximum stress in 1D elements used to model the struts of lattice cells. Table 1 gives the results of the linear static and modal analyses, as well as the final compliance, mass, volume fraction and the range of strut radius used in lattice cells. As Table 1 shows, as a result of topology optimization, depending on the relative density distribution, strut radii in the range of 0.1 mm- 1.5 mm are used in the lattice cells. The total volume given in Table 1 corresponds to a volume fraction of 0.59 which is higher than the 0.5 volume fraction constraint imposed during the topology optimization because of the lattices placed following the topology optimization. It is also noted that the maximum stress in the 1D beam elements used to model the struts of the lattice cells exceed the stress constraint imposed during the topology optimization, since the stress constraint is only active on the 3D elements during the topology optimization.

Table 1: Results of the linear static and modal analyses and the final compliance, mass, volume fraction and the range of strut radius used in lattice cells of the topology optimized wing structure

Result	Initial Lattice Placed and Sized Wing Structure (Minimum Compliance)
Strut Radius (mm)	0.1-1.5
Fundamental Frequency (Hz)	26.05
Compliance (mm/N)	56326.23
Mass (kg)	31.33
Total Volume (mm^3)	11,228,300
Maximum Displacement (mm)	33.23
Maximum von-Mises stress in 2D elements (MPa)	104.1
Maximum von-Mises stress in 3D elements (MPa)	86.08
Maximum von-Mises stress in 1D elements (MPa)	207.6
Volume Fraction	0.59

3.2. Optimization of Srrut Radius of Lattice Cells

At the end of the topology optimization with lattice placement, the resulting strut radii vary from one cell to another depending on the relative density distribution determined. In order to reduce the variability of the strut radius and to ease the manufacturing process of the final wing structure, in this section, for the size optimization process, lattice struts are divided into 5 groups, having equal radii between the defined intervals. The minimum and maximum strut radii were determined as 0.1 mm and 1.50 mm, respectively, after the lattice placement. The grouping of these lattice cell structures are conducted in the intervals given in Equation 4,

Lattice strut radius optimizations are conducted in HyperStudy utilizing the Global Response Surface Method (GRSM) as the optimization algorithm. Before starting the size optimization process, trial optimization runs are conducted to determine the most appropriate starting point and the starting strut radius is taken as 0.5 mm. Size optimizations are first conducted for minimum compliance and mass separately with single objective function, then for minimizing compliance and mass at the same time utilizing a multi-objective function involving compliance and mass as given by Equation 3,

$$\begin{cases} 0.10\ mm \leq r_i \leq 0.38\ mm, & DV1 \\ 0.38\ mm \leq r_i \leq 0.66\ mm, & DV2 \\ 0.66\ mm \leq r_i \leq 0.94\ mm, & DV3 \\ 0.94\ mm \leq r_i \leq 1.22\ mm, & DV4 \\ 1.22\ mm \leq r_i \leq 1.50\ mm, & DV5 \end{cases} \quad (4)$$

Figures 7-9 present the variations of 5 design variables with respect to the number of iterations, for the minimum compliance, minimum mass and minimum compliance and mass. These results shows that in the three different size optimizations, convergence is reached and multi-objective optimization involving both compliance and mass yields radius values between the radius values obtained through single objective optimizations involving compliance and mass only.

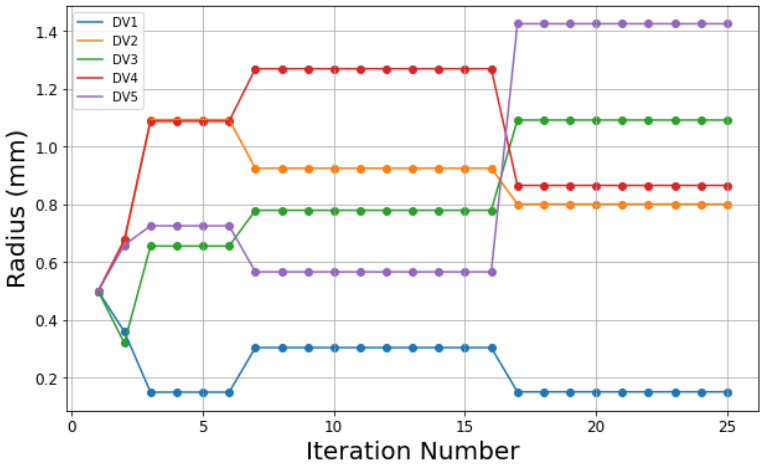

Fig. 7: Variations of design variables with the iteration number for the strut radius optimization of the wing structure with 5 design variables (minimum compliance)

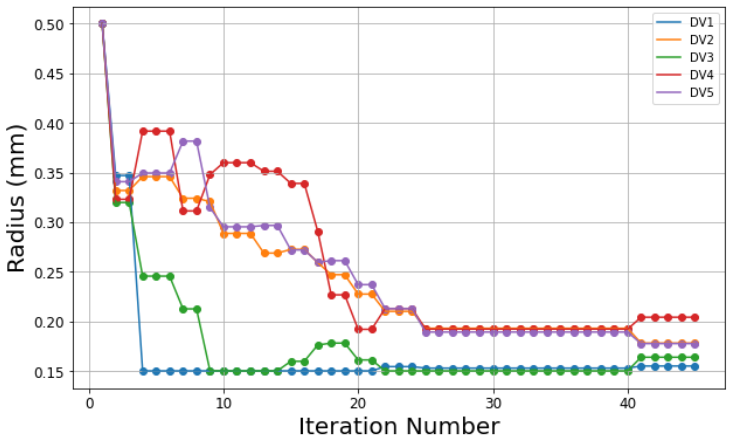

Fig. 8: Variations of design variables with the iteration number for the strut radius optimization of the wing structure with 5 design variables (minimum mass)

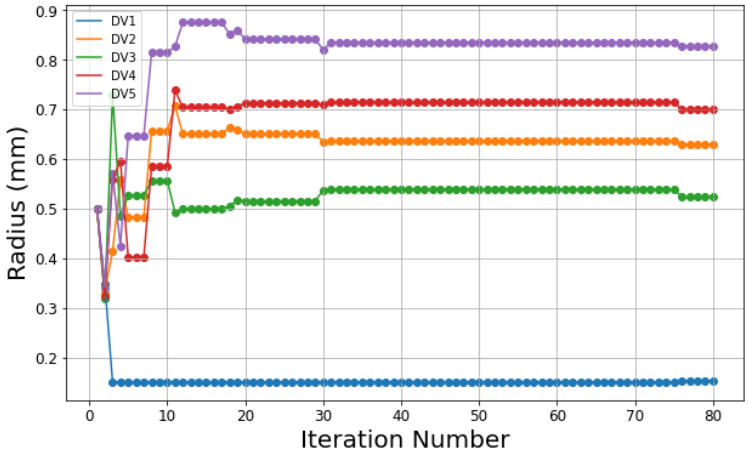

Fig. 9: Variations of design variables with the iteration number for the strut radius optimization of the wing structure with 5 design variables (minimum mass and compliance)

Table 2 compares the optimization results obtained by lattice cell assisted topology optimization and strut radius size optimization with 5 design variables. It is noted that as a result of size optimization, stress constraint is satisfied in all (1D, 2D and 3D) finite elements as opposed to topology optimization for lattice placement. For the minimum mass optimization, the maximum stress reaches the stress constraint of 165 MPa, as expected. The fundamental frequency of the optimized wing structures increases by approximately 4.5 Hz compared to the fundamental frequency of the non-optimized wing. Since the non-optimized wing has the highest mass and the lowest compliance, lower frequency of the non-optimized wing is dominated by the higher mass of the non-optimized wing. For the wing configuration studied, single objective (minimum compliance, minimum mass) and multi-objective (minimum compliance and mass) strut radius optimization results show that, the final mass and compliance values are very close to each other, as well as the maximum displacement and frequency results. Multi-objective optimization involving both compliance and mass yields results between the results obtained through single objective optimizations involving compliance and mass only. As a result of two level optimization performed involving lattice cell assisted topology optimization followed by multi-objective strut radius optimization of lattice cells, approximately 17.5% weight reduction is achieved. Finally, for manufacturability a Python code is developed to automatically generate the optimized wing structure in CATIA environment. Figure 10 shows the cross-section of the lattice region of the wing manufactured by the SLS method utilizing the PA12 material.

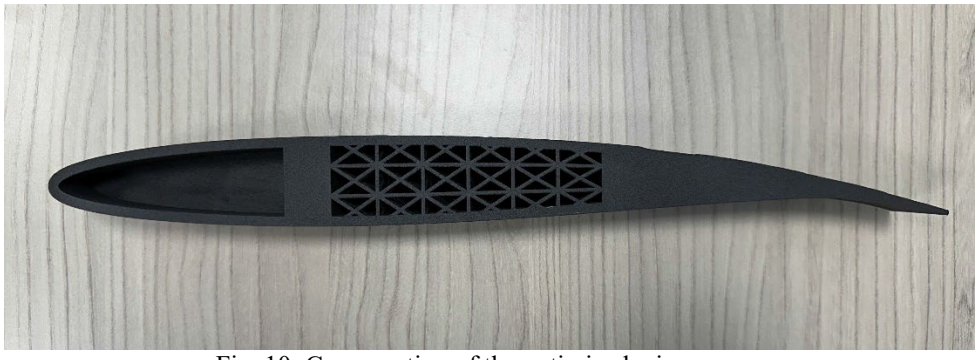

Fig. 10: Cross section of the optimized wing

Table 2: Comparison of topology and strut radius size optimization results

	Non-optimized Wing Structure	Topology Optimization for Lattice Placement	Strut radius Optimization (Minimum Compliance)	Strut radius Optimization (Minimum Mass)	Strut radius Optimization (Multi-Objective)
Design Variable 1 (mm)	N/A	0.1-1.5	0.15	0.15	0.15
Design Variable 2 (mm)	N/A	N/A	0.80	0.18	0.63
Design Variable 3 (mm)	N/A	N/A	1.09	0.16	0.52
Design Variable 4 (mm)	N/A	N/A	0.87	0.20	0.70
Design Variable 5 (mm)	N/A	N/A	1.42	0.18	0.83
Mass (kg)	37.82	31.33	31.41	31.09	31.22
Compliance (mm/N)	53985.01	56236.23	56295.87	56522.25	56381.89
Max. von-Mises Stress in 1D-3D elements (MPa)	104.1	207.60	79.80	165.11	89.15
Max. Displacement (mm)	30.23	33.23	33.20	33.42	33.29
Fundamental Freq. (Hz)	21.55	25.58	26.00	26.04	26.03

4. Conclusion

In this study, a two level optimization strategy is followed for an extendable wing. The two level optimization strategy is based on lattice cell assisted topology optimization followed by size optimization for lattice cells for improving the mechanical performance of the wing structure, as well as achieving weight reduction while satisfying the design constraints. As a result of two level optimization performed involving lattice cell assisted topology optimization followed by multi-objective strut radius optimization of lattice cells, approximately 17.5% weight reduction is achieved. Fundamental frequencies of the optimized wing structures increase by approximately 4.5 Hz compared to the fundamental frequency of the non-optimized wing. For manufacturability a Python code is developed to automatically generate the optimized wing structure in CATIA environment. The developed Phyton code scans the finite element model file containing the optimization results, determines the lattice positions, automatically designs them and creates the CAD model. In this way, the CAD data of the optimized wing structure can be created in the CAD design environment automatically and the necessary modifications can be made quickly.

References

[1] Maconachie, T., Leary, M., Lozanovski, B., Zhang, X., Qian, M., Faruque, O., & Brandt, M. (2019, December). SLM lattice structures: Properties, performance, applications and challenges. *Materials & Design*, *183*, 108137. https://doi.org/10.1016/j.matdes.2019.108137.

[2] Amin Yavari, S., Ahmadi, S., Wauthle, R., Pouran, B., Schrooten, J., Weinans, H., & Zadpoor, A. (2015, March). Relationship between unit cell type and porosity and the fatigue behavior of selective laser melted meta-biomaterials.

Journal of the Mechanical Behavior of Biomedical Materials, *43*, 91–100. https://doi.org/10.1016/j.jmbbm.2014.12.015.

[3] Christensen, J., & de Abajo, F. J. G. (2012, March 23). Anisotropic Metamaterials for Full Control of Acoustic Waves Physical Review Letters, 108(12). https://doi.org/10.1103/physrevlett.108.124301.

[4] Fang, N., Xi, D., Xu, J., Ambati, M., Srituravanich, W., Sun, C., & Zhang, X. (2006, April 30). Ultrasonic metamaterials with negative modulus. *Nature Materials*, *5*(6), 452–456. https://doi.org/10.1038/nmat1644.

[5] Dong, G., Tang, Y., Li, D., & Zhao, Y. F. (2020, May). Design and optimization of solid lattice hybrid structures fabricated by additive manufacturing. Additive Manufacturing, 33, 101116. https://doi.org/10.1016/j.addma.2020.101116.

[6] Liu, Ou, He, & Wen. (2019). Topological Design of a Lightweight Sandwich Aircraft Spoiler. Materials, 12(19), 3225. https://doi.org/10.3390/ma12193225.

[7] Li, D., Liao, W., Dai, N., Dong, G., Tang, Y., & Xie, Y. M. (2018). Optimal design and modeling of gyroid-based functionally graded cellular structures for additive manufacturing. Computer-Aided Design, 104, 87–99. https://doi.org/10.1016/j.cad.2018.06.003.

[8] Teimouri, M., Mahbod, M., & Asgari, M. (2021). Topology-optimized hybrid solid-lattice structures for efficient mechanical performance. Structures, 29, 549–560. https://doi.org/10.1016/j.istruc.2020.11.055.

[9] Boeing Images - Boeing JDAM ER (Extended Range) Kit. (n.d.).https://secure.boeingimages.com/archive/Boeing-JDAM-ER--Extended-Range--Kit-2F3XC5P43Y7.html.

[10] Optistruct user's guide, 13.0, Altair Engineering, Troy, MI.HS-1020: Work with a Parameterized File Model for Size Variables. (n.d.). (C) Copyright 2021. https://2021.help.altair.com/2021/hwdesktop/hst/topics/tutorials/hst/tut_hs_1020_t.htm#tut_hs_1020_t.